Grazing alters sandy soil greenhouse gas emissions in a sand-binding area of the Hobq Desert, China

WANG Bo, LI Yuwei*, BAO Yuhai

College of Geographical Science, Inner Mongolia Normal University, Hohhot 010010, China

Abstract: Deserts are sensitive to environmental changes caused by human interference and are prone to degradation. Revegetation can promote the reversal of desertification and the subsequent formation of fixed sand. However, the effects of grazing, which can cause the ground-surface conditions of fixed sand to further deteriorate and result in re-desertification, on the greenhouse gas (GHG) fluxes from soils remain unknown. Herein, we investigated GHG fluxes in the Hobq Desert, Inner Mongolia Autonomous Region of China, at the mobile (desertified), fixed (vegetated), and grazed (re-desertified) sites from January 2018 to December 2019. We analyzed the response mechanism of GHG fluxes to micrometeorological factors and the variation in global warming potential (GWP). CO_2 was emitted at an average rate of 4.2, 3.7, and 1.1 mmol/(m²•h) and N_2O was emitted at an average rate of 0.19, 0.15, and 0.09 μmol/(m²•h) at the grazed, fixed, and mobile sites, respectively. Mean CH_4 consumption was as follows: fixed site (2.9 μmol/(m²•h))>grazed site (2.7 μmol/(m²•h))>mobile site (1.1 μmol/(m²•h)). GHG fluxes varied seasonally, and soil temperature (10 cm) and soil water content (30 cm) were the key micrometeorological factors affecting the fluxes. The changes in the plant and soil characteristics caused by grazing resulted in increased soil CO_2 and N_2O emissions and decreased CH_4 absorption. Grazing also significantly increased the GWP of the soil (P<0.05). This study demonstrates that grazing on revegetated sandy soil can cause re-desertification and significantly increase soil carbon and nitrogen leakage. These findings could be used to formulate informed policies on the management and utilization of desert ecosystems.

Keywords: grazing; revegetation; re-desertification; greenhouse gases; global warming potential; Hobq Desert

Citation: WANG Bo, LI Yuwei, BAO Yuhai. 2022. Grazing alters sandy soil greenhouse gas emissions in a sand-binding area of the Hobq Desert, China. Journal of Arid Land, 14(5): 576–588. https://doi.org/10.1007/s40333-022-0095-8

1 Introduction

Soil is a major source of atmospheric greenhouse gases (GHGs) in terrestrial ecosystems and can be either a source or a sink in the global carbon cycle (Mosier et al., 1998). Land desertification is a crucial ecological issue that threatens sustainable development. Approximately 25% of the Earth's total land area is affected by desertification. The fragile vegetation and soil systems in these regions affect the stability of the soil carbon pool, leading to the release of sequestered soil carbon, which increases total greenhouse gas (GHG) emissions, which are predominately emitted by industrial fossil fuels, and accelerates global warming (Poulter et al., 2014). Several studies have focused on soil GHG fluxes in forests, wetlands, agricultural lands, and grassland ecosystems (Lohila et al., 2003; Wu and Yao, 2010). Scholars have realized the importance of desert ecosystems in the carbon cycle. In recent years, several studies were conducted on seasonal

*Corresponding author: LI Yuwei (E-mail: liyuwei@imnu.edu.cn)

Received 2022-02-11; revised 2022-04-28; accepted 2022-05-11

changes in GHG fluxes (Wang et al, 2020), environmental and anthropogenic influences (Subke et al., 2003; Liu et al., 2015), and soil respiration components (Castillo-Monroy et al., 2011) in desert ecosystems. Human intervention can lead to complex changes in fragile sand, and scholars have mainly focused on the processes of desertification and vegetation restoration (Wang et al, 2021); however, the subsequent re-desertification of fixed sandy areas is not well understood.

The Hobq Desert is the seventh largest desert in China. The structure and function of the ecosystem in its eastern region have been severely damaged due to several years of cultivation, grazing, and other human intervention. Since the 21st century, forestry authorities have begun to restore the area via artificial vegetation, which has gradually fixed the mobile sand. In this process, regional microhabitats were developed to increase vegetation cover, resulting in the formation of ecosystems and community succession (Búrquez et al., 2010). Furthermore, the soil–vegetation interactions can affect soil physical-chemical traits, root distribution, microbial colonization, and soil fauna activities, promote the development and succession of biological crusts (Hammad et al., 2020), and indirectly change the spatial and temporal patterns in soil GHG fluxes. It has been suggested that artificial vegetation substantially changed the soil–vegetation system and water and temperature equilibriums, leading to altered rates of GHG emissions from sandy soil (Song et al., 2012; Zhang et al., 2013).

Grazing in fixed sandy areas with vegetation cover can yield favorable economic benefits. However, environmental heterogeneity, water shortage, and soil infertility are ongoing problems in newly fixed sandy areas. Therefore, the vegetation has limited resistance and resilience to disturbance and is vulnerable to degradation (Elena et al, 2020). Grazing on such fragile land could result in a sharp reduction in vegetation cover, fragmentation of surface biocrust, and reappearance of bare sand patches on the land surface, resulting in land re-desertification. In typical grasslands, grazing plays an important role in regulating GHG emission and absorption. Grazing changes the plant community composition (Mark, 2020), reduces the accumulation of litter and soil carbon storage, and alters the physical and chemical properties of plants and soils, thus affecting GHG emissions from the grassland ecosystem. However, unlike typical grasslands, it remains unknown how grazing and subsequent changes in the soil microenvironment affect soil GHG emission patterns in fixed sandy areas.

In this study, the effects of sandy soil alteration caused by vegetation restoration and grazing on desert ecosystems were investigated in a sand-binding area of the Hobq Desert. We selected three sites in the area, including mobile (desertified), fixed (vegetated), and grazed (re-desertified) sites. The grazed site had previously been mobile dune sand, which was then vegetated (fixed), but re-desertification occurred due to grazing. The background characteristics of landform and soil of the three sites were homologous, but they have been differentiated due to the interference of human activities, resulting in different landscape features and vegetation types. We aimed to determine the effect of sandy soil changes caused by grazing or revegetation on GHG fluxes, identify the seasonal variations in GHG fluxes, and investigate the micrometeorological factors driving changes in GHG fluxes. The results of this study can provide scientific evidence for the rational utilization and management of desert ecosystems in the context of global climate change.

2 Materials and methods

2.1 Study area and experimental site

The study area is located in the southeast of the Hobq Desert, Inner Mongolia Autonomous Region of China, with a total area of approximately 1.0×10^4 hm^2 and an elevation of 1100–1300 m. The study area has a temperate continental climate with substantial seasonal variation, characterized by hot rainy summers and cold dry winters. The annual average temperature is 8.3 ℃, and the frost-free time is approximately 135 d. The average annual precipitation is 317 mm; rainfall mainly occurs from June to September, which accounts for 84.4% of the annual rainfall. The mean annual evaporation is 2560 mm. The mean annual wind speed is 3.3 m/s, and there is strong wind erosion in this area. The soil types in the study area are mainly aeolian sandy soil formed by aeolian sand

flow deposits. The vegetation is mainly composed of *Salix cheilophila* C.K. Schneid., *Artemisia ordosica* Krasch., and *Caragana korshinskii* Kom.

Human intervention, such as revegetation and grazing, has resulted in dramatic sandy soil changes. Based on a combination of factors, for example, the degree of desertification, the stage of vegetation recovery, the status of surface biocrust development, and the degree of interference, we established the three sites: mobile, fixed, and grazed sites. The mobile site (40°05′46″N, 110°53′38″E) had mobile, bare sand with a low vegetation cover (only a few annual herbs), severe wind erosion, and no biocrust cover on the surface. At the fixed site (40°05′01″N, 110°52′49″E), artificial vegetation has been carried out since 2002 by belt cutting branches of *S. cheilophila*, and the planting specification was 2 m×1 m. Following natural sparsity and artificial rejuvenation, a stable *S. cheilophila* community formed, accompanied by *A. ordosica*, with a high vegetation cover, a thick layer of organic matter on the surface, and the formation of a lichen–moss biocrust with a thickness of 13.2 (±2.1) mm. At the grazed site (40°04′39″N, 110°53′54″E), free grazing began in the spring of 2015, with a grazing intensity of 1.5 sheep/hm^2. Under grazing disturbance, vegetation cover was significantly reduced and the surface biocrust was degraded, with a crust thickness of 8.5 (±1.7) mm. Scattered patches of bare sand began to appear on the surface, indicating that re-desertification was occurring.

2.2 Measurement of greenhouse gas (GHG) fluxes

2.2.1 Variation characteristics of CO_2, N_2O, and CH_4 fluxes

Within each of the three sites, areas with flat terrain and relatively consistent habitats were selected for sampling, and five plots were established. A GHG flux test was conducted over 24 months from January 2018 to December 2019. At each site, one sample was collected at the beginning, middle, and end of each month, that is, for each sampling site, gas samples were collected 360 times during the test period. Soil was collected and the CO_2, N_2O, and CH_4 concentrations were determined using static black box-meteorological chromatography (Hangs et al., 2013). The static black box consisted of a cylindrical top box of 320 mm×600 mm and a pedestal. The top wall was equipped with a stirring fan to evenly mix the gas in the box. The base was placed at the clearing, which was not covered by the *S. cheilophila* canopy, and was at least 1 m away from the base of the plant. We selected all sampling plots according to specific standards to ensure the consistency of basic meteorological elements and to eliminate systematic errors caused by varying distances from plants. The base was pre-embedded into the soil (20 cm) for stability. For sampling, the box was placed in the pedestal groove and water was used to seal the box. Gas sampling was only performed on sunny days. If it was not sunny on a sampling day, sampling was delayed or advanced by one to three days. Sampling took 30 min and was conducted between 09:00 and 12:00 (LST). Gas samples were taken three times, at 0, 15, and 30 min. Because the sampling plots were scattered, we arranged regular personnel at each site in order to ensure the gas collection of the three sample sites can be carried out synchronously, eliminating the error caused by the time difference. The sampling container was a 100 mL syringe with a three-way valve. The gas was stored in an aluminum foil airbag for transportation to the laboratory where the gas concentration was determined within one week. Concentrations of CO_2, N_2O, and CH_4 in the airbags were determined using an Agilent 4890D gas chromatograph (Agilent, Santa Clara, CA, USA).

Diurnal variation in gas flux was observed 11 times in July and August of both 2018 and 2019. Each diurnal change observation began at 06:00, and the gas was collected every 2 h until 04:00 the next day. A total of 12 gas samples were collected in a day.

We calculated the GHG fluxes based on the change in gas concentrations over time (Song et al., 2008). Positive values indicate the emission of GHGs from soil, and negative values represent that the soil absorbs GHGs from the atmosphere. We calculated the gas flux according to the following formula:

$$F = \rho \times h \times \frac{dC}{dt} \times \frac{273}{273+\mathrm{T}}, \quad (1)$$

where F represents the gas flux of CO_2 (mmol/(m^2·h)), CH_4 (μmol/(m^2·h)), and N_2O (μmol/(m^2·h)); ρ is the gas density under standard conditions (kg/m^3); h is the height of the closed static chamber (m); dC/dt is the rate of change in the GHG concentration during measurement; and T is the temperature inside the chamber (℃).

2.2.2 Global warming potential (GWP)

Global warming potential (GWP) is usually used to measure the contribution of different types of GHGs to global warming. GWP is calculated in terms of CO_2 equivalent over a 100-a time scale, and the GWP of CH_4 and N_2O is 28 and 265 times that of CO_2, respectively, i.e., 1 g CH_4/m^2=28 g CO_2/m^2 and 1 g N_2O/m^2=265 g CO_2/m^2 (IPCC, 2014).

2.3 Micrometeorological factors

Micrometeorological factors at the mobile, fixed, and grazed sites were monitored continuously from January 2018 to December 2019. Rainfall was recorded using a small automatic weather station (HOBO U30-NRC, Onset, Bourne, USA) every 30 min. Photosynthetically active radiation (PAR) was measured using a light sensor (HOBO LIA-M003, Onset, Bourne, USA) at a height of 3 m above the ground. Wind speed was measured using a wind sensor (HOBO WSB-M003, Onset, Bourne, USA). Air temperature and humidity were measured using sensors (HOBO S-THB-M002, Onset and HOBO S-THB-M008, Onset, Bourne, USA) at heights of 2.5 and 0.1 m above the ground, respectively. Soil water content was measured using a soil moisture sensor (TDR100, Campbell Scientific, Logan, Germany), at depths of 10, 20, and 30 cm. Soil temperature was measured using a temperature sensor (TCAV, Campbell Scientific, Logan, Germany), at depths of 10, 20, and 30 cm.

Biomass and soil properties of the three sites were investigated at the plot level in August 2018 (Table 1). Three 10 m×10 m shrub plots were set up diagonally in each standard land, and five 1 m×1 m herbaceous plots were randomly selected from each shrub plot to investigate vegetation community characteristics, e.g., plant species, height, coverage, and density. The soil profile was collected by digging into the center of each shrub quadrat, and three soil samples were collected at a depth of 0–20 cm and mixed to form a single composite sample. Samples were taken back to the laboratory for air drying, crushing, and sieving. The external potassium dichromate–sulfuric acid oxidation heating method was used to determine the soil organic carbon. The Kjeldahl method was used to determine soil total nitrogen content. Soil total phosphorus content were determined using an elemental analyzer (FP-LIBS, FELLES, Tianjin, China). The ring-knife method was used to determine the soil bulk density. The quantity of soil microorganisms, including bacteria, actinobacteria, and fungi, was analyzed. An UltraClean DNA Isolation Kit (Mo Bio Laboratories, Solana Beach, CA, USA) was used to extract total microorganism DNA, and a PCR instrument (C1000™ Touch Thermal, Bio-Rad, CA, USA) was used for amplification. Finally, the quantity of microorganisms was estimated via fluorescence ration PCR (CFX96, Bio-Rad, CA, USA).

Table 1 Vegetation biomass, soil physicochemical properties, and soil microorganisms at a soil depth of 0–20 cm

Site	SOM (g/kg)	TN (g/kg)	TP (g/kg)	AN (mg/kg)	AP (mg/kg)	Bulk density (g/cm^3)
Mobile	0.65±0.32^c	0.049±0.250^b	0.37±0.02^b	1.83±0.73^c	2.34±0.16^a	1.61±0.18^a
Fixed	2.53±1.41^a	0.099±0.054^a	0.43±0.04^a	3.19±1.45^b	1.37±0.57^c	1.48±0.11^b
Grazed	0.79±0.41^b	0.042±0.019^b	0.36±0.04^b	4.09±1.92^a	2.13±0.79^b	1.54±0.24^a

Site	Bacteria quantity (10^4/g)	Actinobacteria quantity (10^4/g)	Fungi quantity (10^4/g)	Aboveground biomass (g/m^2)	Root biomass (g/m^2)
Mobile	12.2±1.8^c	6.8±0.5^c	0.10±0.02^c	2.4±0.5^c	1.1±1.3^c
Fixed	711.3±45.8^a	102.6±34.2^a	1.20±0.30^a	566.7±255.4^a	314.1±12.8^a
Grazed	516.3±12.4^b	47.8±3.8^b	0.50±0.02^b	226.9±100.3^b	205.3±23.4^b

Note: SOM, soil organic matter; TN, soil total nitrogen; TP, soil total phosphorus; AN, soil available nitrogen; AP, soil available phosphorus. Different lowercase letters indicate significant differences among the three sites (P<0.05). Mean±SE.

2.4 Statistical analysis

Excel and Origin were used for data processing and visualization, and SPSS 20.0 software was

used for statistical analysis. One-way analysis of variance (one-way ANOVA) and least significant difference (LSD) test were used to determine differences in GHG fluxes among the mobile, fixed, and grazed sites (P=0.05). Two-way analysis of variance (two-way ANOVA) was used to determine the effects of sandy soil changes and season on GHG fluxes. The effects of micrometeorological factors on GHG fluxes were investigated using Pearson's correlation coefficient. Redundancy analysis (RDA) was used to analyze the main factors affecting GHG fluxes in the growing season (from May to October), non-growing season (from November to April of the following year), and the whole study period. A total of 1080 samples of each gas flux were obtained from the three sites during the study period, with 540 each in both the growing season and non-growing season.

3 Results

3.1 Environmental variables in the study area

The average air temperature in the study area in 2018 and 2019 was 8.4 ℃ and 8.3 ℃, respectively. Cumulative precipitation was 333.2 mm in 2018 and 369.6 mm in 2019. Soil temperature (0–20 cm) in the study area was 0.2 ℃ lower in 2018 than in 2019, and soil water content was 5.7% higher in 2018 than in 2019 (Fig. 1). Significant differences in soil temperature and soil water content were detected among the three sites. Soil temperature at the mobile site was higher than that at the fixed and grazed sites by 36.5% and 19.3%, respectively. The mobile site also exhibited the highest soil water content, and was 17.8% and 27.3% higher than that of the fixed and grazed sites, respectively.

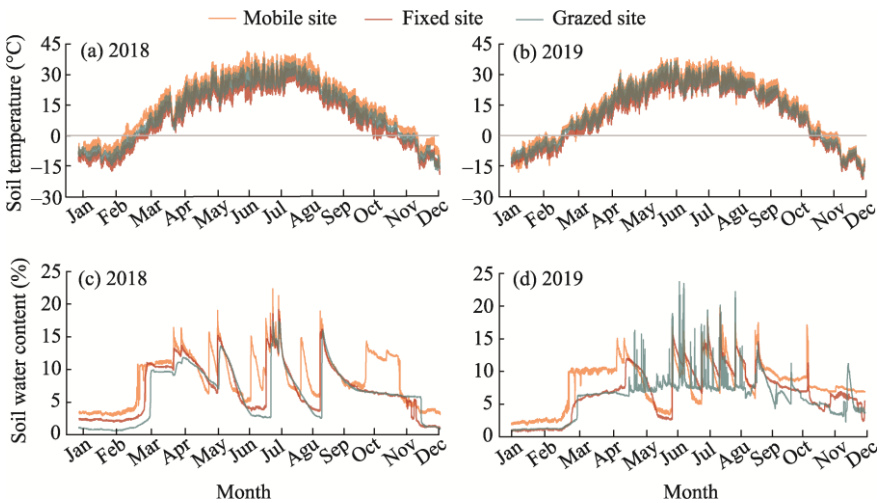

Fig. 1 Fluctuations of soil temperature (a and b) and soil water content (c and d) at the mobile, fixed, and grazed sites in the Hobq Desert in 2018 and 2019

3.2 Spatial and temporal variations in GHG fluxes

The CO_2, N_2O, and CH_4 fluxes in 2018 and 2019 are shown in Figures 2 and 3. Emissions of CO_2 and N_2O were detected from the mobile, fixed, and grazed sites, whereas CH_4 absorption occurred at all sites. However, GHG fluxes varied significantly among the sites. The CO_2 emission flux followed the order of grazed site (4.2 mmol/(m^2·h))>fixed site (3.7 mmol/(m^2·h))>mobile site (1.1 mmol/(m^2·h)); the N_2O emission flux followed the order of grazed site (0.19 μmol/(m^2·h))>fixed site (0.15 μmol/(m^2·h))>mobile site (0.09 μmol/(m^2·h)); and the CH_4 absorption flux followed the order of fixed site (2.9 μmol/(m^2·h))>grazed site (2.7 μmol/(m^2·h))>mobile site (1.1 μmol/(m^2·h)). No significant differences were detected in GHG fluxes between 2018 and 2019, but significant seasonal variations were observed. At the three sites, CO_2 emissions were the highest in summer and the lowest in winter. At the mobile site, N_2O was briefly absorbed in the winter. Similar to the

other two sites, N_2O emissions were greater in spring and summer, and more CH_4 was absorbed in spring and summer, but the absorption volume decreased significantly in autumn and winter.

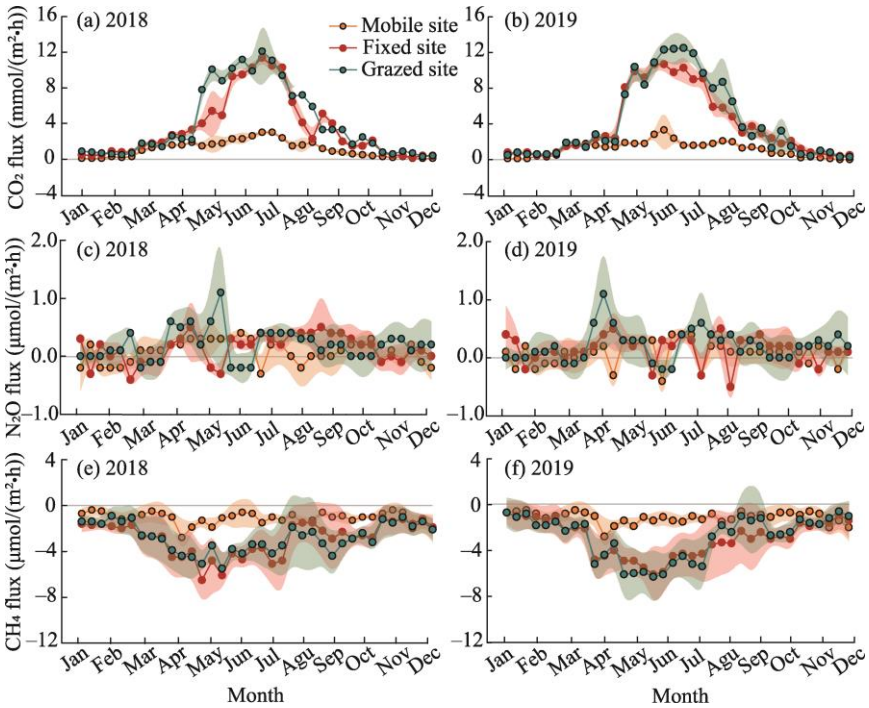

Fig. 2 Fluctuations of CO_2 (a and b), N_2O (c and d), and CH_4 (e and f) fluxes at the mobile, fixed, and grazed sites in the Hobq Desert in 2018 and 2019. The shaded area is the standard error of the five plots measured at each site.

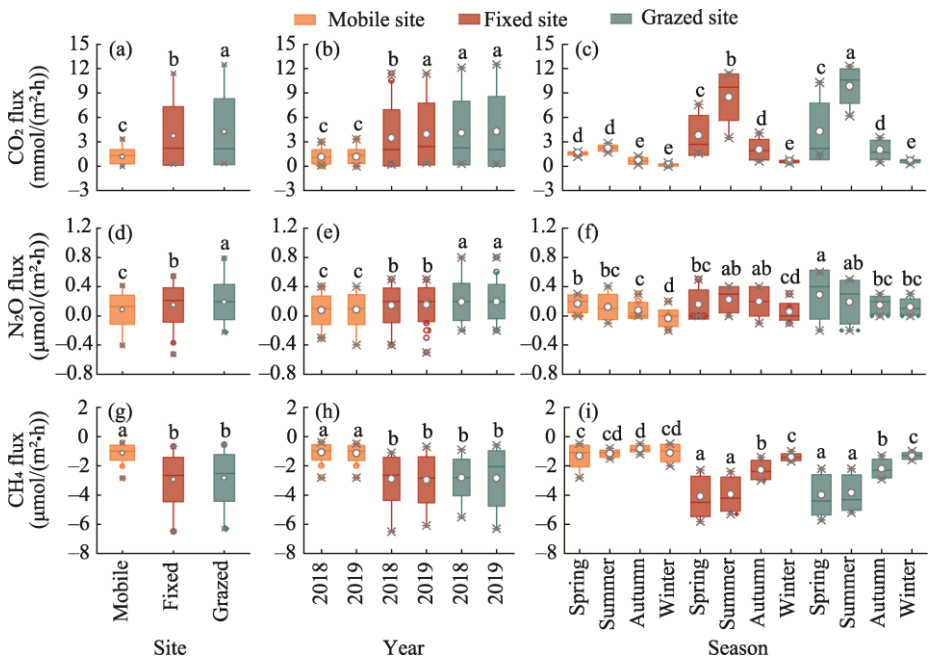

Fig. 3 Mean, annual, and seasonal CO_2 (a–c), N_2O (d–f), and CH_4 (g–i) fluxes at the mobile, fixed, and grazed sites in the Hobq Desert during 2018–2019. The boxes represent the range from the lower quantile (Q25) to the upper quantile (Q75). The dots and horizontal lines inside the boxes represent the means and medians, respectively. The dots outside the boxes represent outliers. The upper and lower whiskers indicate the maximum and minimum values, respectively. Different lowercase letters indicate significant differences in gas fluxes (P<0.05).

CO_2, N_2O, and CH_4 fluxes exhibited daily variation patterns, and the fluxes were all greater in the daytime than in the nighttime (Fig. 4). For the mobile, fixed, and grazed sites, CO_2 emissions were the highest between 10:00 and 12:00. The N_2O emissions were the highest from 14:00 to 16:00 at the mobile site, from 10:00 to 12:00 at the fixed site, and from 12:00 to 14:00 at the grazed site. The absorption of CH_4 was the greatest from 16:00 to 18:00 at the mobile site, and from 12:00 to 14:00 at both the fixed and grazed sites.

Results of the two-way ANOVA revealed that sandy soil changes, season, and their interaction significantly affected CO_2 and CH_4 fluxes (P<0.01; Table 2). The partial η^2 indicated that CO_2 flux was more affected by season than by sandy soil changes, whereas the effect of sandy soil changes on CH_4 flux was significantly greater than that of season. N_2O flux was not affected by sandy soil changes; however, N_2O flux exhibited seasonal variations.

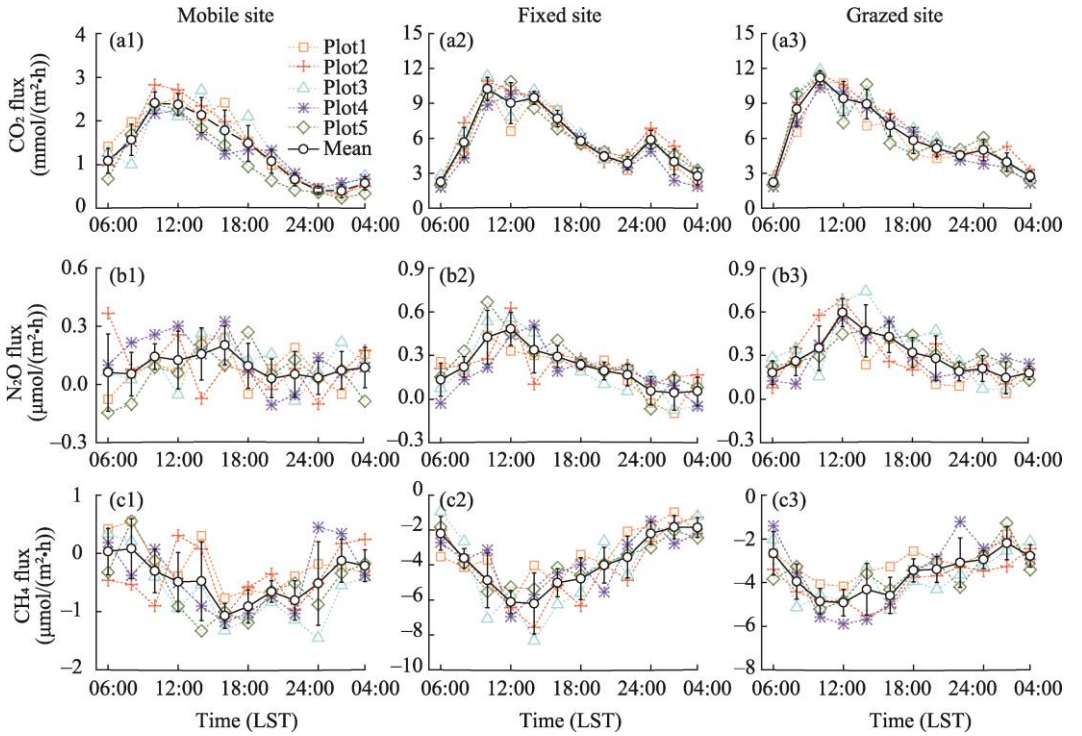

Fig. 4 Daily fluctuations of CO_2 (a1–a3), N_2O (b1–b3), and CH_4 (c1–c3) fluxes at the mobile, fixed, and grazed sites in the Hobq Desert. Mean±SE.

Table 2 Effects of sandy soil changes, season, and their interaction on CO_2, N_2O, and CH_4 fluxes

Item	Source of variation	Sum of square	*df*	Mean square	*F* value	*P* value	Partial η^2
	Sandy soil changes	174.062	2	87.031	31.247	0.000**	0.394
CO_2 flux	Season	590.847	3	196.949	70.711	0.000**	0.688
	Sandy soil changes×Season	132.654	6	22.109	7.938	0.000**	0.332
	Sandy soil change	0.231	2	0.115	2.523	0.086	0.050
N_2O flux	Season	0.581	3	0.194	4.234	0.007**	0.117
	Sandy soil changes×Season	0.504	6	0.084	1.838	0.100	0.103
	Sandy soil change	73.567	2	36.783	48.401	0.000**	0.502
CH_4 flux	Season	48.889	3	16.296	21.443	0.000**	0.401
	Sandy soil changes×Season	20.070	6	3.345	4.401	0.001**	0.216

Note: *df*, degree of freedom. ** indicates that the difference between treatments is extremely significant at the 0.01 level.

3.3 Variations in soil GWP

There were significant differences in GHG fluxes among the mobile, fixed, and grazed sites. The grazed site exhibited the highest CO_2 and N_2O emissions, and the fixed site had the highest CH_4 absorption (Fig. 5). The grazed site had the highest GWP (1597.7 g $CO_2/(m^2 \cdot a)$), followed by the fixed site (1401.6 g $CO_2/(m^2 \cdot a)$) and the mobile site (440.8 g $CO_2/(m^2 \cdot a)$).

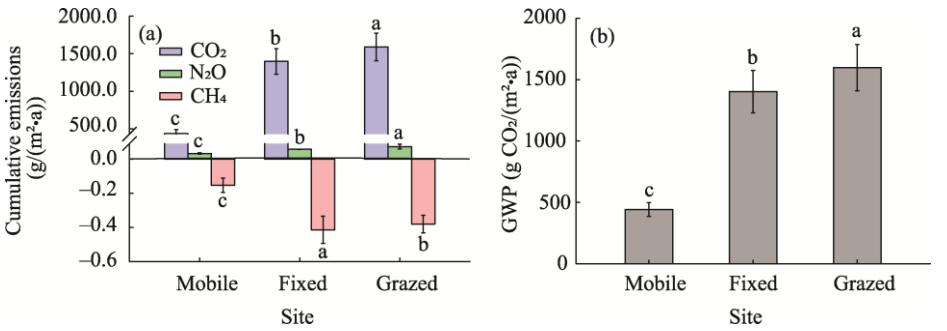

Fig. 5 Cumulative emissions of CO_2, N_2O, and CH_4 (a) and global warming potential (GWP, b) at the mobile, fixed, and grazed sites in the Hobq Desert. Different lowercase letters indicate significant differences among the three sites (P<0.05). Mean±SE.

3.4 Correlations between micrometeorological factors and GHG fluxes

To determine the effects of micrometeorological factors on CO_2, N_2O, and CH_4 fluxes, we performed the Pearson's linear regression analysis (Fig. 6) and redundancy analysis (Fig. 7). The linear regression analysis showed that CO_2 flux at the mobile, fixed, and grazed sites had a significant positive correlation with atmospheric, surface, and soil temperatures at each depth. Soil water content, rainfall, and PAR were also significantly positively correlated with CO_2 flux. N_2O flux at the grazed site was significantly positively correlated with rainfall, whereas it was not correlated with temperature. At the fixed site, N_2O flux was significantly positively correlated with the surface soil water content (10 cm), but not with any other variables (Fig. 6). In contrast, N_2O flux at the mobile site was significantly correlated with temperature, soil water content, and PAR. At the fixed and grazed sites, CH_4 flux was significantly negatively correlated with humidity and atmospheric, surface, and soil temperatures at each depth. CH_4 flux at the mobile site was significantly correlated with the deep soil water content (30 cm), but not with any other variables.

According to the results from Figure 7, during the growing season, the cumulative contribution of the first (soil water content at a depth of 30 cm, SWC-30) and second (surface soil temperature, T-10) principal components was 83.2% (Fig. 7a). The former explained 40.5% of the variation and the latter explained 24.5% of the variation. The mobile site was distinctly separated along RDA1, showing a positive relationship of fluxes with soil water content and soil moisture in the lower layer. During the non-growing season, the cumulative contribution of the first (SWC-30) and second (PAR) principal components was 87.6% (Fig. 7b). The former explained 51.4% of the variation and the latter explained 13.1% of the variation. CH_4 flux was significantly and negatively correlated with SWC-30 and PAR, which are consistent with the results of linear correlation analysis. The three sites had comparable micrometeorological characteristics.

Over the study period, the cumulative contribution of the first (T-10) and second (SWC-30) principal components was 81.3% (Fig. 7c). The former explained 40.9% of the variation and the latter explained 14.5% of the variation. There was no separation among the three sites.

4 Discussion

4.1 Effects of revegetation on GHG fluxes

This study shows that revegetation of a sand-binding area can significantly increase soil CO_2 emissions. Revegetation resulted in higher coverage of shrubs and grasses and greater aboveground

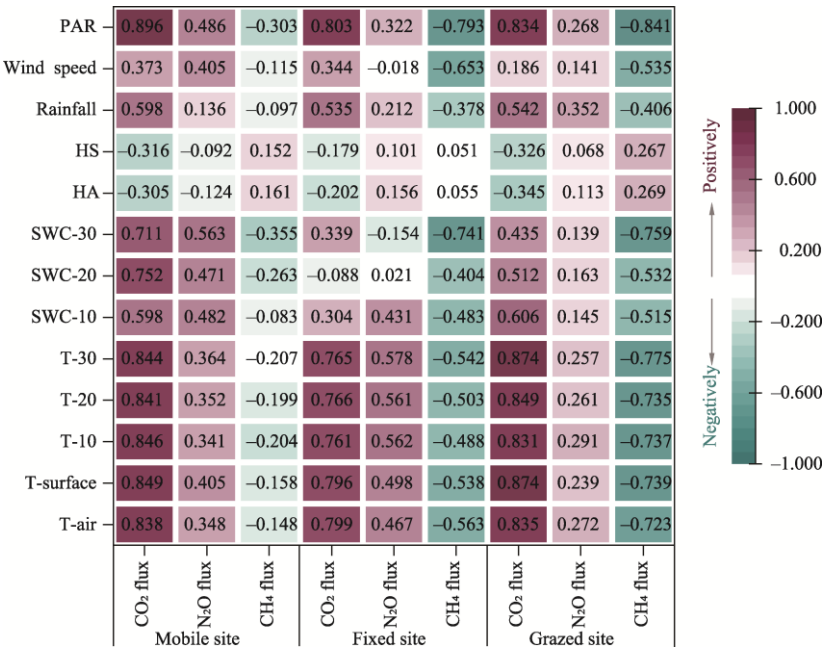

Fig. 6 Results of Pearson's linear correlation analysis between GHG fluxes (CO_2, N_2O, and CH_4 fluxes) and micrometeorological factors at the mobile, fixed, and grazing sites. The numbers in the boxes are the Pearson correlation coefficients. PAR, Photosynthetic active radiation; HS, humidity of surface; HA, humidity of air; SWC-30, soil water content at 30 cm depth; SWC-20, soil water content at 20 cm depth; SWC-10, soil water content at 10 cm depth; T-30, soil temperature at 30 cm depth; T-20, soil temperature at 20 cm depth; T-10, soil temperature at 10 cm depth; T-surface, surface temperature; T-air, air temperature.

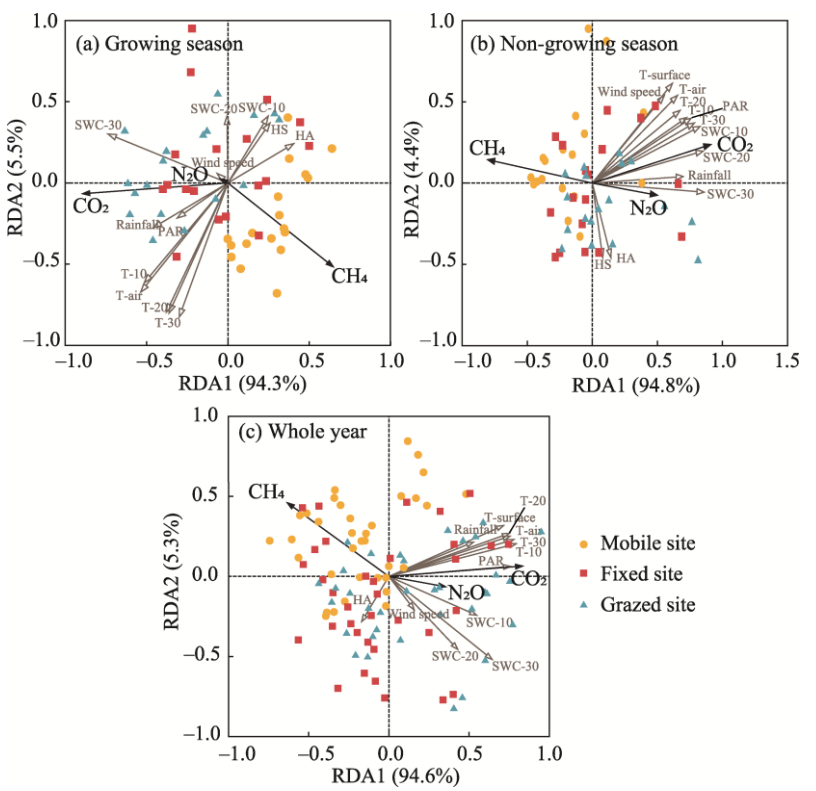

Fig. 7 Redundancy analysis of GHG fluxes and micrometeorological factors during the growing season (a), non-growing season (b), and whole year (c)

and belowground biomass (Table 1). The synergistic effects of soil–vegetation systems caused spatial heterogeneity of soil CO_2 flux in desert soils to a large extent, and soil respiration was significantly enhanced with vegetation restoration and biocrust development. The primary sources of CO_2 emissions from sandy soil are plant root respiration, cryptogam respiration in biocrust, soil microbial respiration, and soil animal respiration (Cable et al., 2011). Autotrophic respiration is performed by living plant roots, and dead plant roots are a substrate for heterotrophic respiration by soil microorganisms; therefore, root growth can improve soil aeration (Rustad et al., 2000). Consequently, increased root biomass will increase CO_2 emissions. An increase in aboveground biomass means that the canopy covers a larger area, where it can effectively regulate microclimate and condense soil resources, forming "fertility islands" under shrubs, creating ideal conditions for the formation and colonization of biocrust (Hu et al., 2002). Castillo-Monroy et al. (2011) reported that biocrust autotrophic respiration was the main contributor to respiration in desert soil, accounting for up to 42% of the total respiration. In this study, a mixed crust had developed at the fixed site, explaining why the CO_2 emissions from the fixed site were significantly greater than those from the mobile site. Soil–vegetation interactions can directly affect soil factors and thus indirectly affect soil CO_2 emissions. Soil organic matter and total nitrogen content were significantly higher at the fixed site (Table 1), which can also explain the higher CO_2 emissions from this site. Soil organic carbon is a substrate for biological growth. Soils with high organic carbon contents generally have higher biological activities and thus higher respiration rates (Priess et al., 2001). Nitrogen is an important component of amino acids, proteins, nucleotides, and coenzymes, and can directly affect photorespiration and root cell mitochondrial respiration (Fitter et al., 1999). Soil bacteria, fungi, and actinomycetes use soil organic matter in heterotrophic respiration. The higher microbial biomass at the fixed site could also explain the higher CO_2 emissions.

The air permeability of sandy soil provides an ideal aerobic environment for nitrifying bacteria, explaining why sandy soil is often a source of N_2O emissions. In this study, N_2O emission rate of the fixed site was greater than that of the mobile site. Vegetation restoration reduces soil compactness, creating an ideal environment for the proliferation of microorganisms, thereby increasing autotrophic or heterotrophic nitrification and subsequent N_2O emissions (Wolf and Russow, 2000). Additionally, soil organic carbon and nitrogen are essential for nitrification; chemotrophic nitrifying bacteria use soil organic carbon as an energy source and oxidize NH_4^+ or organic compounds to form N_2O and other N-containing gases (Papen and Rennenberg, 1990). Therefore, the increased soil organic carbon and total nitrogen contents at the fixed site also explained the higher N_2O emissions.

In this study, the sandy soil at all sites absorbed CH_4. In the process of vegetation restoration, improvements to micrometeorological and environmental conditions can gradually increase the amount of CH_4 absorbed by soil. Methane-oxidizing bacteria generally oxidize and consume CH_4 in soil under aerobic conditions. Under anaerobic conditions, fiber-decomposing bacteria and methane-producing bacteria in the soil produce CH_4 and release it into the atmosphere (van den Pol-van Dasselaar and Oenema, 1999; Yu et al., 2006). At the fixed site, the increase in aboveground biomass produced a better shading effect and promoted the development of mixed crusts, resulting in good soil aeration. Meanwhile, the increase in plant root biomass also increased soil porosity and decreased soil bulk density (Table 1). This higher porosity likely led to greater air permeability, thereby promoting oxidation (and thus absorption) of CH_4.

4.2 Effects of grazing on GHG fluxes

Grazing has two effects on the regulation of GHGs: (1) it changes the carbon pool of the ecosystem and thus has a direct impact on GHG emissions (Jones et al., 2017); and (2) it indirectly affects the exchange of ecosystem and atmospheric GHGs by changing soil physical, chemical, and biological properties (Zhou et al., 2010). However, after reviewing the literature, we found that the effects of grazing on soil GHG emissions varies with climate conditions and soil physicochemical properties (Howden et al., 1994; Wang et al., 2003; Soussana et al., 2007; Dunmola et al., 2010; Zhou et al., 2011; Shi et al., 2017). In this study, grazing increased CO_2

emissions. In grasslands, livestock grazing usually does not degrade the surface soil, but can decrease the belowground biomass and reduce the soil respiration rate. However, in deserts, the soil surface is fragile and vegetation and biocrust can easily be destroyed by livestock, exposing organic carbon to the surface where it can be oxidized into CO_2 and emitted into the atmosphere (Cao et al., 2012).

The effects of grazing on N_2O flux also vary considerably among previous studies (Table 3). Most studies on grasslands show that grazing does not significantly affect N_2O emissions, and that seasonal dynamics as well as source and sink patterns do not fluctuate significantly. However, in the present study, grazing increased N_2O emissions from sandy soil. This could be attributed to the loose structure of the soil, which can be easily compacted under livestock trampling, resulting in a higher soil bulk density, reduced soil porosity (Table 1), limited oxygen diffusion, and reduced oxygen concentration in the soil. These factors could result in a higher denitrification rate under anaerobic conditions (Douglas and Crawford, 1993), thus promoting N_2O emissions. Furthermore, livestock excrement is a primary source of N_2O (de Klein et al., 2014). Deposition and decomposition of livestock excrement add nitrogen to the soil. An increase in N_2O substrates increases nitrification and, subsequently, N_2O emissions.

Similar to most previous studies (Table 3), we found that grazing reduced soil absorption of CH_4. Grazing increased the surface soil bulk density, leading to a decrease in the water-holding capacity. This likely led to increased seepage resistance and decreased gas diffusion, resulting in anaerobic microsites where CH_4 could be produced.

Table 3 Comparison of the effects of grazing on CO_2, N_2O, and CH_4 fluxes of different land use types

Location	Land type	Precipitation (mm)	Temperature (℃)	CO_2 emissions	N_2O emissions	CH_4 absorption	Reference
China	Semi-arid grassland	460	2.8	Reduced	Unchanged	Reduced	Wang et al. (2003)
China	Desert grassland	372	7.3	Increased	Unchanged	Reduced	Zhou et al. (2011)
China	Desert steppe	350	7.5	Reduced	Increased	Increased	Shi et al. (2017)
Canada	Temperate grassland	970	6.2	Unchanged	Unchanged	Reduced	Chai et al. (2015)
Australia	Tropical typical steppe	750	12.5	Reduced	Increased	Increased	Howden et al. (1994)
Hungary	Semi-natural grassland	500	10.5	Reduced	Unchanged	Reduced	Soussana et al. (2007)
France	Temperate grassland	1310	8.0	Reduced	Reduced	Reduced	Soussana et al. (2007)
China	Fixed sandy land	317	8.3	Increased	Increased	Reduced	This study

4.3 Factors controlling GHG fluxes

Pearson's linear correlation and Redundancy analysis revealed that T-10 and SWC-30 had the most significant influence on GHG emissions. GHG fluxes at the mobile, fixed, and grazed sites were significantly affected by seasonal changes. GHG fluxes followed a similar trend to soil water content and temperature, being high in spring and summer but low in autumn and winter. This trend was consistent across all sites. GHG emissions and absorption are the products of soil bio-metabolism and biochemical processes, which are sensitive to water and temperature conditions. Within a specific range, an increase in soil temperature can accelerate the decomposition of organic matter, increasing plant roots and soil microorganism metabolism rates, and thus increasing GHG emissions from soil (Brito et al., 2015). However, at extremely low (<5 ℃) or high temperatures (>40 ℃), root activity, methanogenesis, and nitrification are inhibited (Yu et al., 2006), which explain the lower GHG fluxes in autumn and winter. In this study, in both growing and non-growing seasons, the soil water content at 30 cm had a significantly higher effect on GHG fluxes than those at other soil depths, potentially because the roots of the dominant species (*S. cheilophila* and *A. ordosica*) dominated the 20–40 cm soil layer. Soil water content affects soil permeability, pH, microbial activity, and the gas diffusion rate, which are closely related to plant root distribution (Chimner and Cooper, 2003). High soil water content can also

alter root structure and increase root exudates which, in turn, increase soil carbon and soil microbial activity (de Vries et al., 2019), thereby increasing GHG emissions.

5 Conclusions

In this study, the ecosystem of the sand-binding area was still highly fragile, human activities such as vegetation restoration or grazing have resulted in dramatic sandy soil changes. Grazing on vegetated sand will destroy vegetation and significantly increase soil carbon and nitrogen leakage. The grazed site had the highest emissions of CO_2 and N_2O and the highest GWP. The GHG fluxes and GWP at the mobile site were the lowest. The fixed site had the largest CH_4 uptake. Across the three sites, soil temperature at a depth of 10 cm and soil water content at a depth of 30 cm were the key micrometeorological factors determining GHG fluxes. The findings of this study illustrate that revegetation and grazing have caused significant sandy soil changes and altered GHG fluxes and GWP. Furthermore, we determined the specific role of re-desertification caused by grazing, highlighting the need for a comprehensive understanding of GHG fluxes in such environments to facilitate rational exploitation of desert land resources.

Acknowledgements

The study was supported by the Inner Mongolia Science and Technology Project of China (2022YFDZ0027) and the Mongolia Basic Geographical Factors and Land Use/Cover Survey of China (2017FY101301-4).

References

Brito L F, Azenha M V, Janusckiewicz E R, et al. 2015. Seasonal fluctuation of soil carbon dioxide emission in differently managed pastures. Agronomy Journal, 107(3): 957–962.

Búrquez A, Martínez-Yrízar A, Núñez S, et al. 2010. Aboveground biomass in three Sonoran Desert communities: Variability within and among sites using replicated plot harvesting. Journal of Arid Environments, 74(10): 1240–1247.

Cable J M, Ogle K, Lucas R W, et al. 2011. The temperature responses of soil respiration in deserts: a seven desert synthesis. Biogeochemistry, 103: 71–90.

Cao L H, Liu H M, Zhao S W, et al. 2012. Relationship between carbon and nitrogen in degraded alpine meadow soil. African Journal of Agricultural Research, 7(27): 3945–3951.

Castillo-Monroy A P, Maestre F T, Rey A, et al. 2011. Biological soil crust microsites are the main contributor to soil respiration in a semiarid ecosystem. Ecosystems, 14(5): 835–847.

Chimner R A, Cooper D J. 2003. Influence of water table levels on CO_2 emissions in a Colorado subalpine fen: an *in situ* microcosm study. Soil Biology and Biochemistry, 35(3): 345–351.

de Klein C A M, Shepherd M A, van der Weerden T J. 2014. Nitrous oxide emissions from grazed grasslands: interactions between the N cycle and climate change—a New Zealand case study. Current Opinion in Environmental Sustainability, (9–10): 131–139.

de Vries F T, Williams A, Stringer F, et al. 2019. Changes in root-exudate-induced respiration reveal a novel mechanism through which drought affects ecosystem carbon cycling. The New Phytologist, 224(1): 132–145.

Douglas J T, Crawford C E. 1993. The response of a ryegrass sward to wheel traffic and applied nitrogen. Grass and Forage Science, 48(2): 91–100.

Dunmola A S, Tenuta M, Moulin A P, et al. 2010. Pattern of greenhouse gas emission from a Prairie Pothole agricultural landscape in Manitoba, Canada. Canadian Journal of Soil Science, 90(2): 243–256.

Elena V, Gulya K, Rauan Z, et al. 2020. Can conservation agriculture increase soil carbon sequestration? A modelling approach. Geoderma, 369: 114298, doi: 10.1016/j.geoderma.2020.114298.

Fitter A H, Self G K, Brown T K, et al. 1999. Root production and turnover in an upland grassland subjected to artificial soil warming respond to radiation flux and nutrients, not temperature. Oecologia, 120(4): 575–581.

Hammad H M, Nauman H M F, Abbas F, et al. 2020. Carbon sequestration potential and soil characteristics of various land use systems in arid region. Journal of Environmental Management, 264: 110254, doi: 10.1016/j.jenvman.2020.110254.

Hangs R D, Schoenau J J, Lafond G P. 2013. The effect of nitrogen fertilization and no-till duration on soil nitrogen supply power and post-spring thaw greenhouse-gas emissions. Journal of Plant Nutrition and Soil Science, 176(2): 227–237.

Howden S M, White D H, Mckeon G M, et al. 1994. Methods for exploring management options to reduce greenhouse gas emissions from tropical grazing systems. Climatic Change, 27(1): 49–70.

Hu C X, Liu Y D, Song L R, et al. 2002. Effect of desert soil algae on the stabilization of fine sands. Journal of Applied

Phycology, 14(4): 281–292.
IPCC. 2014. Mitigation of Climate Change. Working Group III Contribution to the Fifth Assessment Report of the Intergovernmental Panel on Climate Change. In: Edenhofer O, Pichs-Madruga R, Sokona Y, et al. Cambridge and New York: Cambridge University Press.
Jones S K, Helfter C, Anderson M, et al. 2017. The nitrogen, carbon and greenhouse gas budget of a grazed, cut and fertilised temperate grassland. Biogeosciences, 14: 2069–2088.
Liu Q, Zhao C, Cheng X, et al. 2015. Soil respiration and carbon pools across a range of spruce stand ages, eastern Tibetan Plateau. Soil Science and Plant Nutrition, 61(3): 440–449.
Lohila A, Aurela M, Regina K, et al. 2003. Soil and total ecosystem respiration in agricultural fields: effect of soil and crop type. Plant and Soil, 251(2): 303–317.
Mark E R. 2020. Grazing management, forage production and soil carbon dynamics. Resources, 9(4): 49, doi: 10.3390/resources9040049.
Mosier A R, Delgado J A, Keller M. 1998. Methane and nitrous oxide fluxes in an acid Oxisol in western Puerto Rico: effects of tillage, liming and fertilization. Soil Biology and Biochemistry, 30(14): 2087–2098.
Papen H, Rennenberg H. 1990. Microbial processes involved in emissions of radiatively important trace gases. In: Transactions 14th International Congress Soil Science. Kyoto, 2: 232–237.
Poulter B, Frank D, Ciais P, et al. 2014. Contribution of semi-arid ecosystems to interannual variability of the global carbon cycle. Nature, 509: 600–603.
Priess J A, de Koning G H J, Veldkamp A. 2001. Assessment of interactions between land use change and carbon and nutrient fluxes in Ecuador. Agriculture, Ecosystems and Environment, 85(1–3): 269–279.
Qi Y S, Dong Y S, Zhang S. 2002. Methane fluxes of typical agricultural soil in the North China Plain. Journal of Ecology and Rural Environment, 18(3): 56–58, 60. (in Chinese)
Rustad L E, Huntington T G, Boone R D. 2000. Controls on soil respiration: Implications for climate change. Biogeochemistry, 48(1): 1–6.
Shi H Q, Hou L Y, Yang L Y, et al. 2017. Effects of grazing on CO_2, CH_4, and N_2O fluxes in three temperate steppe ecosystems. Ecosphere, 8(4): e01760, doi: 10.1002/ecs2.1760.
Song C C, Zhang J B, Wang Y Y, et al. 2008. Emission of CO_2, CH_4 and N_2O from freshwater marsh in northeast of China. Journal of Environmental Management, 88(3): 428–436.
Song W M, Chen S P, Wu B, et al. 2012. Vegetation cover and rain timing co-regulate the responses of soil CO_2 efflux to rain increase in an arid desert ecosystem. Soil Biology and Biochemistry, 49: 114–123.
Soussana J F, Allard V, Pilegaard K, et al. 2007. Full accounting of the greenhouse gas (CO_2, N_2O, CH_4) budget of nine European grassland sites. Agriculture Ecosystems and Environment, 121(1–2): 121–134.
Subke J A, Reichstein M, Tenhunen J D. 2003. Explaining temporal variation in soil CO_2 efflux in a mature spruce forest in Southern Germany. Soil Biology and Biochemistry, 35(11): 1467–1483.
van den Pol-van Dasselaar A, Oenema O. 1999. Methane production and carbon mineralisation of size and density fractions of peat soils. Soil Biology and Biochemistry, 31(6): 877–886.
Wang B, Duan Y X, Wang W F, et al. 2020. Desertification reversion alters soil greenhouse gas emissions in the eastern Hobq Desert, China. Environmental Science and Pollution Research, 27(13): 15624–15634.
Wang B, Liu J, Zhang X, et al. 2021. Changes in soil carbon sequestration and emission in different succession stages of biological soil crusts in a sand-binding area. Carbon Balance and Management, 16(1): 27, doi: 10.1186/s13021-021-00190-7.
Wang Y S, Hu Y Q, Ji B M, et al. 2003. An investigation on the relationship between emission/ uptake of greenhouse gases and environmental factors in semiarid grassland. Advances in Atmospheric Sciences, 20(1): 295–310.
Wolf I, Russow R. 2000. Different pathways of formation of N_2O, N, and NO in black earth soil. Soil Biology and Biochemistry, 32(2): 229–239.
Wu X, Yao Z S, Brüggemann N, et al. 2010. Effects of soil moisture and temperature on CO_2 and CH_4 soil–atmosphere exchange of various land use/cover types in a semi-arid grassland in Inner Mongolia, China. Soil Biology and Biochemistry, 42(5): 773–787.
Yu K W, Chen G X, Xu H. 2006. Rice yield reduction by chamber enclosure: a possible effect on enhancing methane production. Biology and Fertility of Soils, 43(2): 257–261.
Zhang Z S, Li X R, Nowak R S, et al. 2013. Effect of sand-stabilizing shrubs on soil respiration in a temperate desert. Plant and Soil, 367(1–2): 449–463.
Zhou P, Han G D, Wang C J, et al. 2011. Effects of stocking rates on carbon flux in the desert grassland ecological system of Inner Mongolia. Journal of Inner Mongolia Agricultural University (Natural Science Edition), 32(4): 59–64. (in Chinese)
Zhou Z C, Gan Z T, Shangguan Z P, et al. 2010. Effects of grazing on soil physical properties and soil erodibility in semiarid grassland of the Northern Loess Plateau (China). CATENA, 82(2): 87–91.